Identification of highly potent and selective MMP2 inhibitors addressing the S1' subsite with D-proline-based compounds

Elena Lenci,[a] Riccardo Innocenti,[a] Tommaso Di Francescantonio,[a] Gloria Menchi,[a,b] Francesca Bianchini,[b,c] Alessandro Contini,[d] Andrea Trabocchi[a,b,*]

[a] *Department of Chemistry "Ugo Schiff", University of Florence, Via della Lastruccia 13, 50019 Sesto Fiorentino, Florence, Italy*

[b] *Interdepartmental Center for Preclinical Development of Molecular Imaging (CISPIM), University of Florence, Viale Morgagni 85, 50134 Florence, Italy*

[c] *Department of Clinical and Experimental Biomedical Science "Mario Serio", University of Florence, Largo Brambilla 3, 50134 Florence, Italy*

[d] *Department of Pharmaceutical Sciences, University of Milan, Via Venezian 21, I-20133 Milan, Italy*

* Corresponding author. Phone, +39 055 4573507; fax, +39 055 4574913; E-mail, andrea.trabocchi@unifi.it.

ABSTRACT

MMP2 and MMP9, also called gelatinases, play a primary role in the angiogenic switch, as a fundamental step of tumor progression, and show high degree of structural similarity. Clinically successful gelatinase inhibitors need to be highly selective as opposite effects have been found for the two enzymes, and the S1' subsite is the major driver to attain selective and potent inhibitors. The synthesis of D-proline-derived hydroxamic acids containing diverse appendages at the amino group, varying in length and decoration allowed to give insight on the MMP2/MMP9 selectivity around the S1' subsite, resulting in the identification of sub-nanomolar compounds with high selectivity up to 730. Molecular docking studies revealed the existence of an additional hydrophobic channel at the bottom of S1' subsite for MMP2 enzyme useful to drive selectivity towards such gelatinase.

Keywords: Peptidomimetics; Amino acids; Enzyme inhibition; Angiogenesis; Matrix metalloproteinase; Drug discovery

Introduction

Therapies targeting angiogenesis and metastasis hallmarks are continuously being studied for many malignancies, and among the many different molecular targets, matrix metalloproteinases (MMPs) are receiving a renewed interest, not only for the development of new drugs, but also as diagnostic and prognostic biomarkers.[1] Matrix metalloproteinases (MMPs) are a family of zinc-dependent neutral endopeptidases,[2] that are key players in the turnover and remodeling of the extracellular matrix (ECM) on both normal and pathological processes. Approximately 23 members of MMP family have been known in human,[3] and these MMPs can be divided into six categories.[4] Gelatinases A (MMP2) and B (MMP9) mainly digest denatured collagens and are involved in a number of pathological events leading to cancer, as well as inflammatory diseases, cardiovascular diseases, and neurological disorders.[5] Gelatinases play a primary role in the angiogenic switch, as a fundamental step of tumor progression.[6] The degradation of extracellular matrix components facilitate the angiogenesis and tumor cell invasiveness, which is a phenotypic feature of malignancy essential to perform different steps of the metastatic cascade. Several pro-angiogenic factors, such as the vascular endothelial growth factor (VEGF)[7] and the transforming growth factor beta (TGF-β),[8] immobilized on tumor cells and endothelial cells surface, are released by the action of these MMPs. During tumor progression a complex interplay interaction between tumor and stromal cells involving MMPs is

arranged, and most studies show a negative association between MMPs and prognosis.[9] In particular, during the progression of melanoma, as one of the most aggressive human malignancies, MMP2 and MMP9 levels result positively correlated with a negative prognosis.[10] MMP2 directly modulates melanoma cell adhesion and spreading to ECM, suggesting that MMP2 facilitates migration and invasion.[11] Several types of MMPs inhibitors, mainly consisting of the hydroxamate Zn-binding group have been developed during last decades,[12] also including cyclic scaffolds bearing subsite-addressing appendages,[13] sulfonylated amino acid hydroxamates,[14] and proline derivatives.[15] The serious dose-limiting side effects occurring in clinical trials,[16] probably due to the non-selective inhibitory activity, have underlined the importance to identify novel inhibitors able to discriminate among MMPs.[17] In fact, to be clinically successful, MMP inhibitors need to be highly selective for a particular MMP without provoking adverse systemic effects,[18] and in particular, the selective inhibition of gelatinases is of relevance for a successful clinical trial, targeting tumor progression.[19] In particular, MMP2 is considered to be a better candidate target for anticancer drugs than MMP9, whose inhibition is related to drug side effects,[20] and considered as an antitarget in advanced stages of cancer.[18] In this context, despite the high structural similarity of the two gelatinases, recent efforts to the design of MMP2 inhibitors with selectivity over MMP9 and other metalloproteinases have been reported,[21] as well as new insights about the major structural determinants for inhibition selectivity.[22] Nevertheless, the goal of achieving a potent MMP2 inhibitor with high selectivity over the MMP9 gelatinase has still to be achieved.

Following previous application of D-proline-derived peptidomimetics as inhibitors of the Zn-metalloproteinase *Anthrax* lethal factor,[23] we envisaged the application of such concept molecular scaffold in targeting MMP2 and MMP9.[21b] Specifically, we developed additional compounds of this class with aim of developing novel gelatinase inhibitors for subsequent applications in molecular imaging of tumors and as a candidate inhibitor in angiogenesis drug discovery. In this work the elaboration of such compounds is reported, particularly addressing the substitution at the nitrogen atom to study the determinants of inhibition potency and selectivity of gelatinases at the S1' subsite. Taking advantage of D-proline as a cyclic template, a functional group scan was arranged on the amine function to explore the interactions within S1' subsite, based on the length and the chemical functions linking 1 to 3 rings within the *N*-arylsulfonyl moiety.

Results and Discussion

MMP2 and MMP9 gelatinases present high similarity in the protein structure, especially in their catalytic clefts. The structural similarity of the two enzymes was studied with respect to their primary structure and the overall three-dimensional conformation.

3D Structural alignment. We investigated the structural similarity between MMP2 and MMP9 protease, and the key structural features around the active site characterized by S1, S1' and S2/S2' motifs by a three-dimensional structural superimposition of the proteases using molecular modeling (Figure 1). The Swiss PDB viewer (SPDBV) program (4.0.1 version, Swiss Institute of Bioinformatics) was used to superimpose three dimensional (3D) structures of the metalloproteinases taking into account the alpha-carbon atoms of the two proteins.[24] The 3D structure superimposition (RMSD on alpha-carbon of 1.33 Å) demonstrated the two proteins share the same fold, with slight differences around the S1' subsite, as reported.[22a]

Pairwise sequence alignment. The pairwise sequence alignment and a structural superimposition were carried out on MMP2 and MMP9 to give insight about similarity around key subsites. The local alignment performed using the EMBOSS water sequence alignment tool, EMBL-EBI,[25] highlighted a high similarity between the two proteins. Indeed, MMP2 and MMP9 show a similarity and identity of 72.4% and 59.5%, respectively (Figure 2). Residues 120-130 of MMP2, belonging to the catalytic domain S2+S2' show high similarity with the corresponding residues found in the catalytic domain of MMP9, and so as for the S1 cavity (84-86 residues of MMP2). The sequence analysis highlighted that there exist differences between MMP2 and MMP9 in the S1' pocket (140-152 residues of MMP2), which has been recognized as crucial for the

ligand-protein interaction.[26] Indeed, the S1' pocket of MMP9 showed higher degree of hydrophobic nature with respect to that of MMP2.

Fig. 1. Superimposition of MMP2 (PDB: 1HOV, green) and MMP9 (PDB: 1GKC, purple). Both fittings have been obtained with SPDBV.

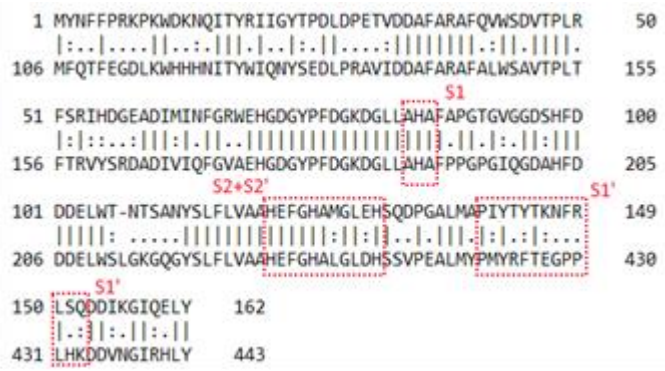

Fig. 2. Pairwise alignment of MMP2 (top, PDB: 1HOV) and MMP9 (bottom, PDB: 1GKC). Key subsites of the two proteins are highlighted with a red dotted frame. Vertical lines represent identity, colon marks represent similarity. MMP9 (1GKC) sequence chain number after G215 continues with Q391.

Synthesis. Suitably substituted phenylsulfonamido compounds containing a 4-methoxy or 3,4-dichloro substituents were initially prepared as reference compounds based on previously reported compounds.[21b] D-proline methyl ester was reacted with the selected arylsulfonyl chloride to give the corresponding sulfonamido esters **2** and **4** in 71% and 78% yield, respectively, following a slight modification of the published procedure reported for L-proline.[27] The methyl ester of such compounds was successively converted to the corresponding hydroxamic acids using NH_2OK/NH_2OH in MeOH to produce the corresponding compounds **3** and **5** in yields ranging from 21% to 36%. (Scheme 1). The development of compounds containing two phenyl rings at the sulfonamido appendage was envisaged through a biphenyl moiety or by means of an acetylene moiety separating the two aromatic rings. Such approach was addressed using cross coupling reactions applied to compound **6**, containing the 4-Br-phenylsulfonyl appendage at the amino group (Scheme 2). Accordingly, compound **6** was synthesized in 72% yield, and subjected to the Sonogashira reaction with phenylacetylene, resulting in the achievement of adduct **7** in 47% yield, and of compound **8** as hydroxamic acid after aminolysis with NH_2OK/NH_2OH in MeOH, as above reported. The

reaction of **6** under Suzuki conditions with 3,4-dichlorophenylboronic acid gave the corresponding diphenyl adduct **9** in 75% yield, and the corresponding hydroxamic acid **10** after reaction of the ester group with NH_2OK/NH_2OH in MeOH in 39% yield. Unfortunately, the Suzuki reaction with styrylboronic acid did not produce the corresponding an additional compound bearing a stilbene appendage (data not shown).

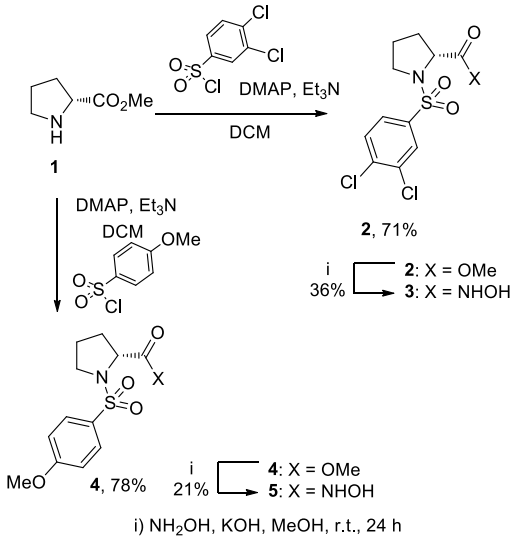

Scheme 1. Synthesis of hydroxamic acids **3** and **5** with single ring appendage.

The functionalization of D-proline methyl ester with a 4-nitrophenylsulfonyl group was considered as a further diversification of the appendage addressing S1' to install two aromatic rings linked by an amide bond (Scheme 3). Thus, the p-nitrobenzenesulfonyl derivative **11**, easily prepared from the corresponding sulfonyl chloride in 89% yield,[28] was hydrogenated under Pd/C catalysis to achieve the corresponding aniline derivative **12** in quantitative yield. This compound was then subjected to acylation with a number of different reactants, to give compounds **13-16** in variable yields. Specifically, acylation with benzoyl chloride and 4-nitrobenzoyl chloride resulted in compounds **13** and **14** with 80 and 59% yields, respectively. The amine protection as Cbz group gave compound **15** in 58% yield, and reaction with Cbz-protected 4-methylaminobenzoyl chloride resulted in the quantitative achievement of compound **16**, containing three aromatic rings at the hydrophobic appendage addressing the S1' subsite. Aminolysis with NH_2OK/NH_2OH in MeOH resulted in the final compounds **17-20** with 29-39% yields, in agreement with previous data about low performance of this transformation. CLogP values for all final compounds were computed and found to be compliant to Lipinski's Ro5 rule (see Table S2 in the Supplementary Data).

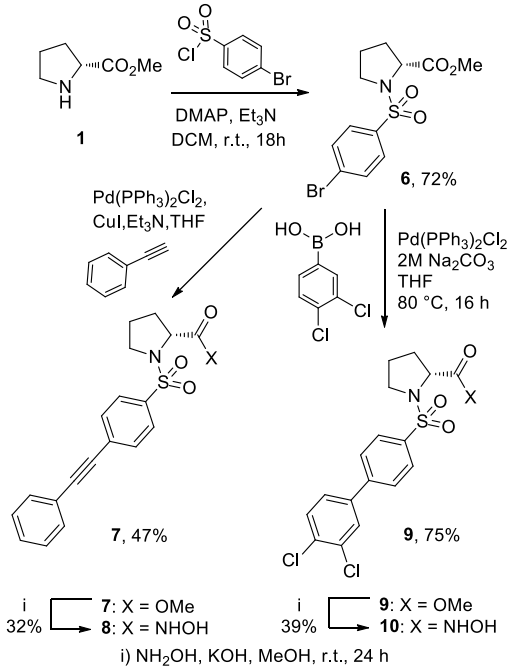

Scheme 2. Synthesis of hydroxamic acids **8** and **10** containing diphenylacetylenyl and biphenyl moieties, respectively.

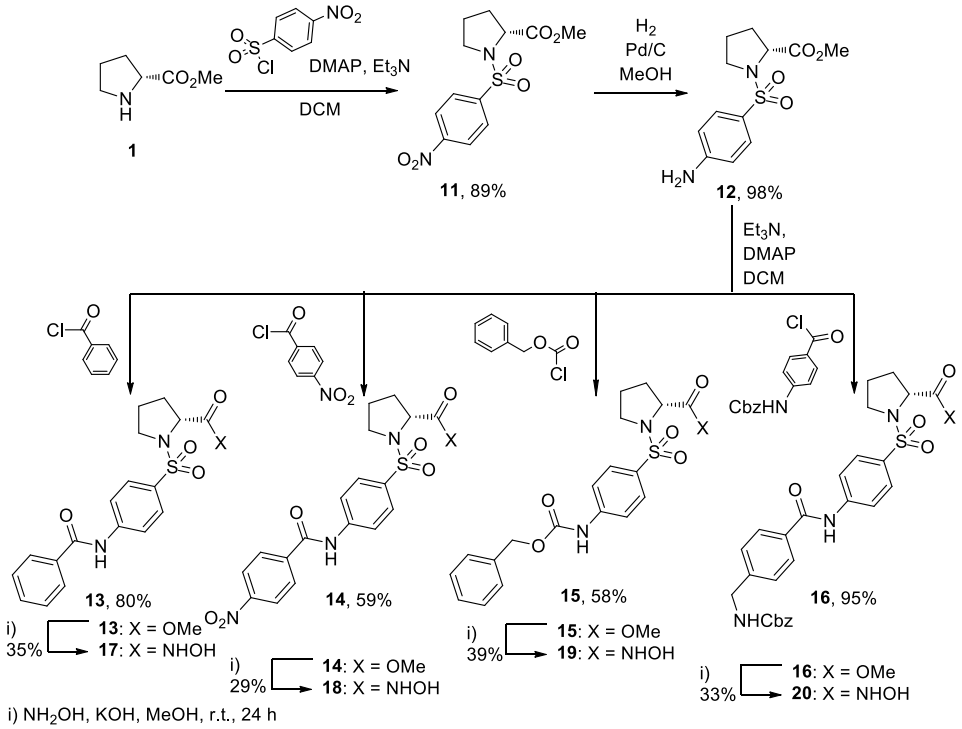

Scheme 3. Synthesis of hydroxamic acids **17-20** containing two to three phenyl rings linked by amide and carbamate bonds.

For all the compounds IC_{50} values were obtained by dose-response measurements using an inhibitor range of concentrations (0.01 nM-20 μM) and enzyme concentration equal to 1 nM.

The inhibition activities of the synthesized compounds towards the two gelatinases, reported in Table 1, suggest the key role of the hydrophobic substituent in determining the enzyme inhibition potency and selectivity. This pool of compounds showed a general preference for the inhibition towards MMP2, contrarily to what previously reported for other D-proline derivatives containing the 3,4-dichlorophenyl moiety addressing the S1' subsite, and a second variable hydrophobic group on the pyrrolidine ring.[21b] This suggested that the sulfonamide group at the nitrogen atom of the proline moiety is the major driver for the selectivity towards the two gelatinases. Reference compounds **3** and **5**, containing a single variably substituted phenyl ring, showed different inhibition potency, with the former possessing poor micromolar activity, and compound **5** displaying inhibition activity in the low nanomolar range. Also, both compounds displayed poor MMP2/MMP9 selectivity, suggesting the edge of the S1' subsite of the two enzymes not possessing significant structural differences. The arylsulfonyl appendage characterized by two phenyl rings, either directly linked or separated by an acetylenyl moiety, showed better inhibition activity, as demonstrated by IC_{50} values for compounds **8** and **10** in the sub-nanomolar range, though still not displaying significant enzyme selectivity. Compounds **17**-**20**, characterized by the presence of an amide bond at the hydrophobic appendage addressing S1' subsite, showed interesting data. Specifically, compound **17**, possessing two phenyl rings linked by an amide bond, displayed inhibition activity for both gelatinases in the nanomolar range, whereas compound **18**, containing an additional nitro group at para position of the second ring, showed a 200- and 400-fold increase in the inhibition potency towards MMP2 and MMP9, respectively, as compared to **17**, though without displaying any enzyme selectivity. Compounds **19** and **20**, characterized by the presence of two or three phenyl rings, respectively, and by the presence of a terminal carbobenzyloxy group, showed very interesting inhibition selectivity for MMP2 enzyme. Specifically, compound **19** proved to strongly inhibit both MMP2 and MMP9 with IC_{50} values of 48 pM and 35 nM, showing a 730-fold selectivity for the former enzyme. In the case of compound **20**, possessing two phenyl rings, inhibition of MMP2 remained in the low nanomolar range, whereas the potency towards MMP9 dropped to low micromolar, although high 218-fold selectivity for MMP2 was still experienced. Given the high inhibition of MMP2 in low nanomolar IC_{50} values for compounds **18**, **19**, and **20**, such compounds were selected for further cell-based investigations, given the major role of gelatinases in angiogenesis and melanoma cell invasion.

Cell based assays. We tested the effect of compounds **18**, **19**, and **20** on cell viability using the MTT tetrazolium assay in parallel with TBE (trypan blue exclusion) assay. The MTT assay is based on the conversion of the MTT dye to a formazan by the action of mitochondrial reductase of living cells and the amount of the measured formazan is directly proportional to the number of cells.

Table 1. Binding activity data of D-proline-derived compounds determined using a fluorogenic peptide substrate.

Cmpd	Structure	IC_{50} MMP 2, nM	IC_{50} MMP 9, nM	MMP9 / MMP2 selectivity	Cmpd	Structure	IC_{50} MMP 2, nM	IC_{50} MMP 9, nM	MMP9 / MMP2 selectivity
3	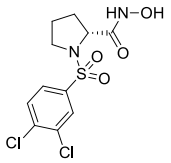	492	4370	8.9	17	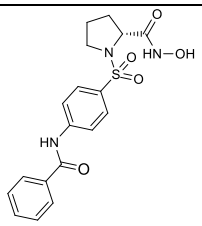	21	47	2.2
5	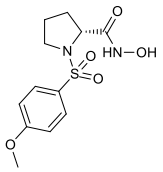	8.9	22	2.5	18	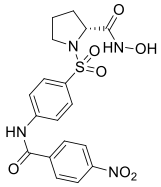	0.096	0.122	1.3
8	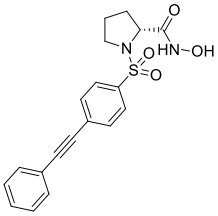	0.28	0.91	3.3	**19**	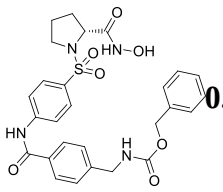	**0.048**	**35**	**730**
10	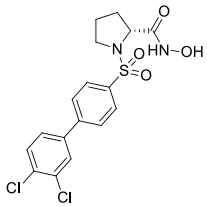	0.16	0.76	4.8	**20**	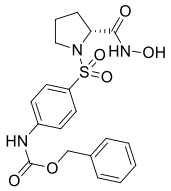	**2.38**	**520**	**218**

The mitochondrial activity and, consequently, the amount of formazan might be downregulated in cells exposed to the different agents, even in the absence of direct damage to cell integrity. Since one of the best markers for cell death is the breakdown of the plasma membrane, we decided to evaluate cell integrity using TBE assay. MCF7 cells derived from the pleural effusion of a metastatic breast adenocarcinoma, express a low metastatic potential in vivo and a lower secretion of activated forms of MMPs, compared to the higher invasive MDA-MB 231 breast cancer cells or A375M6 melanoma cells.[29] We found that compounds **18**-**20** did not induce a cytotoxic effect after a 24 h exposure in MCF7 and no signs of cell death were either found using TBE assay (see Supplementary data). Colon carcinoma aggressiveness strongly correlates with MMPs expression;[30] in particular, it is reported that HCT116 colon carcinoma cells express MMPs, which strongly correlates with cell invasion.[31] As revealed by the results of MTT and TBE assays, in HCT116 cells compounds **18**-**20** showed an extremely faint effect of cell viability. On the other hand, A375M6 melanoma cells, which are known to express high level of both gelatinase A and B,[32] showed a different behavior. In

this case, the MTT assay revealed that the compounds (50 nM to 5 μM range), partially interfered with melanoma cell viability. Interestingly, we found that the inhibitors used in the indicated range, did not induce any effect on cell integrity, as confirmed by the TBE assay. Thus, we might suggest that the reduction in formazan production might depend on the interference with melanoma cell homeostasis rather than an acute damage or a toxic effect.

We further explored the role of compounds **18**-**20** on cell migration and invasiveness using Boyden chambers assay (Figure 3). We exposed A375M6 melanoma cells to different concentration of the three compounds, during a 6 h migration assay. We used the broad range inhibitor Ilomastat (10 μM) as internal control.[33] We found that, at 10 μM concentration, the inhibitory effect of the compounds was significantly stronger as compared to that obtained in melanoma cells exposed to equimolar doses of Ilomastat. Interestingly, at 1 μM concentration, the effect of **19** inhibitor was similar to that of Ilomastat, while the effect of **18** and **20** was still significant, compared to the treatment with Ilomastat. According to previous results, a 6 h exposure treatment excludes that the reduced number of invaded cells may depend on a reduction of cell proliferation.

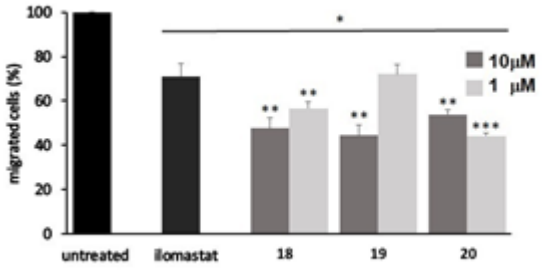

Fig. 3 Effect of the three different compounds on A375M6 invasion through Matrigel. Cells were allowed to migrate through Matrigel coated filters for 6h in the presence of complete 24h-growing media and in the presence of the three different compounds. Bars indicate Mean ± SEM of the percentage of invasive cells/chamber normalized to the untreated cells ($n = 5$). *$p < 0.005$ compared to untreated cells, **$p < 0.01$ and ***$p < 0.001$ compared to ilomastat (10 μM) treated cells.

Taken together, these results highlight that the newly synthesized inhibitors, and in particular the two compounds **20** and **18**, might have an important role in the inhibition of cancer progression not only by the direct inhibition of MMP2 gelatinolytic activity, but also through the inhibition of the multiple biological activities in which MMP2 is involved. Indeed, along with its gelatinolytic activity, MMP2 co-localizes and interacts with many different cell receptors,[34] activates other membrane bound MMPs (in particular proMMP9) and finally, releases growth factors stored in extracellular matrix.[35] Since the MMP2 inhibitors trigger both invasiveness and cell survival, additional experiments will be necessary to unravel the effect of the inhibitors on specific biological activity, overcoming MMP2 pleiotropic activity. Overall, we suggest that, in highly invasive and high MMPs-expressing melanoma cells, compounds **18** and **20**, undertake their action reducing cell viability and invasiveness, while in low MMPs-expressing cells the same results were absent.

Molecular Docking. Docking studies were performed on active compounds **18**-**20** and the reference compound **5** to investigate the major determinants towards the enzymes binding sites, and to assess the structural elements crucial for potency and selectivity towards the two gelatinases. The crystal structures of MMP2 (PDB code: 1HOV) and MMP9 (PDB code: 1GKC) were used to derive optimal receptor models. For the former target, computed binding energies for the top-poses, as well as energies averaged on the top 5 poses, well resemble the experimental outcome, with **19** standing above the others in terms of potency

(Table 2 and Table S1, Supplementary data). Conversely, this compound seems not to be able to efficiently bind to MMP9, where computed binding energies drop by about 3 kcal/mol. Unfortunately, in the case of MMP9, the predicted ranking does not completely reflect the experiments. This is not surprising. Indeed, while pose prediction by docking is rather mature, ranking is still far from being universally reliable.[36] Nevertheless, our computational data identify **5** and **18** as the least selective inhibitors, and **19** as the most selective. Thus, calculations can be considered reliable enough to speculate on the reasons for the observed selectivity.

Table 2. Predicted binding energies (kcal/mol) for ligands **5**, **18**-**20**

	MMP2		**MMP9**	
	top pose	Avg. top 5	top pose	Avg. top 5
5	-10.5	-10.3±0.2	-11.0	-11.0±0.1
18	-12.5	-12.5±0.0	-13.5	-12.7±0.8
19	-14.5	-14.1±0.3	-11.9	-11.1±0.6
20	-12.3	-12.2±0.1	-13.5	-11.8±1.4

MMP2 docking poses for compounds **5**, **18-20** show a main cluster of conformations characterized by the typical binding mode of hydroxamate-based inhibitors (see Supplementary data), with the oxygen atoms of the hydroxamic group chelating the catalytic zinc ion. Moreover, the hydroxamic moiety establishes additional hydrogen bonds with the oxygen side chain of Glu202 and with the amide group of Ala165. In most of the low energy conformations of compounds **18-20** the sulfonamide group experiences typical hydrogen bonding interactions with Leu83 and Ala84, contributing to the correct positioning of the inhibitor within the active site. For compound **5** only, the top-pose do not present a correct positioning of the SO_2 moiety. However, the second-ranked pose, differing by the top-pose by 0.2 kcal/mol (see Table S1, Supplementary data), and poses 3-5, which have comparable binding energy, present the expected binding mode. The presence of the sulfonamido group in MMPs inhibitors is important not only for the establishment of hydrogen bonds with residues belonging to the catalytic site, but also to direct the hydrophobic substituents to the deep and highly hydrophobic S1' subsite.

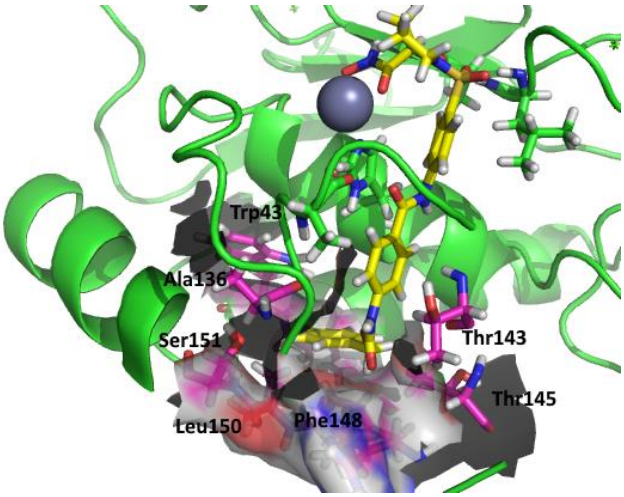

Fig. 4 Compound **19** (yellow) docked into the active site of MMP2 (PDB: 1HOV), highlighting protein residues (purple) that form key interactions within the additional hydrophobic channel.

The published version of this article is available at:

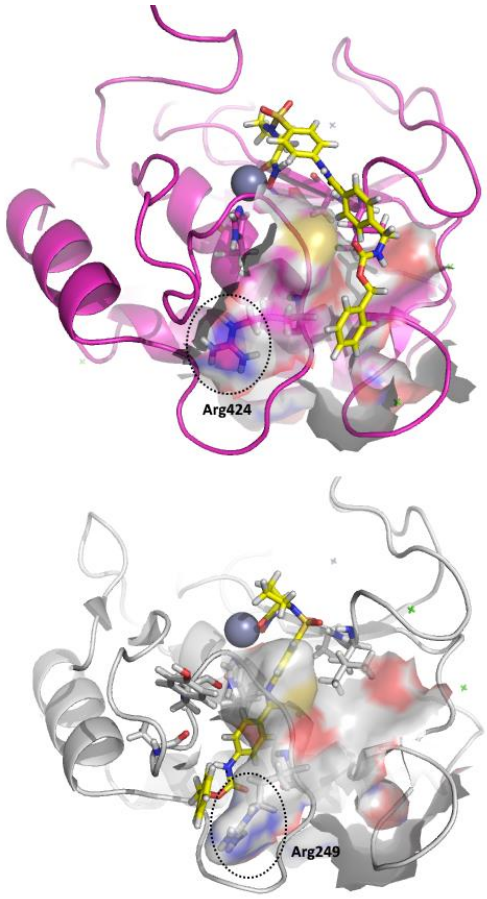

Fig. 5 Top: compound **19** (yellow) docked into the active site of MMP9 (PDB: 1GKC), highlighting Arg424 in closed conformation at the bottom of the S1' subsite; bottom: compound **19** (yellow) docked into the active site of MMP9 (PDB: 4H3X), highlighting Arg249 in open conformation at the bottom of the S1' subsite.

Concerning the most selective inhibitors as of Table 1, visual inspection of the poses justified the preference for MMP2, since this enzyme possesses an additional hydrophobic channel where the chains of **19** and **20** are placed. Such hydrophobic channel formed by Val42, Trp43, Leu137, Phe148, Leu150 particularly well addresses the benzyl ring of **19**, establishing hydrophobic and □-stacking interactions with Val42, Leu137, Leu150 and Trp43, Phe148, respectively (Figure 4, and Figure S2, Supplementary data). This stabilizing interaction is not evinced for MMP9. Indeed, the S1' site in MMP9 is less accessible and is not able to accommodate the large hydrophobic moiety of **19** and, to a lesser extent, of **20**. Accordingly, molecular docking calculations on MMP9 using 1GKC and 4H3X crystallographic structures highlighted the role of an Arg residue at the bottom of S1' subsite (Arg424 for 1GKC and the corresponding residue Arg249 for 4H3X with different residue numbering). In particular, Arg424 can act as a gate that can open and close the hydrophobic subsite. Indeed, compound **19** was found addressing the flexibility of MMP9 at S1', interacting with these two conformational preferences of MMP9 with different binding modes. Specifically, compound **19** show interactions in S1' subsite for open conformation and outside S1' for the closed one (see Figure 5, bottom and top, respectively). The equilibrium between these two energetically different binding poses might then determine the experimentally observed inhibition potency. Such steric clash is not possible in MMP2, where Thr143 is found in place of Arg at the bottom of the S1' subsite (Figure 4), thus justifying the observed selectivity.

Additional insights for rationalizing the reason for such behaviour can be found by comparing the sequences of MMP2 and MMP9 at the S1' site. Figure 6 shows the alignment, where the amino acids that are close (< 4.5 Å) to the predicted binding pose of **19** to MMP2 are highlighted.

Fig. 6 Alignment of the S1' regions of MMP2 (top) and MMP9 (bottom). Amino acids that are at < 4.5 Å to the predicted binding pose of **19** to MMP2 are highlighted.

In addition to the Arg residue mentioned above, a difference between the two sequences that might affect the S1' site is related to the KNFR motif of MMP2, that in MMP9 is replaced by EGPP. Indeed, the two prolines provoke a bending of S1' external loop toward the inner side of the receptor, de facto reducing the volume of the S1' subsite and preventing the accommodation of larger ligands (Figure S3, Supplementary data).

Conclusions

During tumor angiogenesis different molecules interact closely with each other to facilitate tumor progression and metastatic diffusion. It has been demonstrated that gelatinases play an important role in melanoma progression through its co-localization with $\alpha_v\beta_3$ integrin and MT1-MMP in correspondence of the invasive front of the tumor. In this view, our purpose was to identify a class of gelatinase inhibitors from a pool of hydroxamic acid-containing peptidomimetics derived from D-proline, and containing a key hydrophobic group for suitable interactions with flanking S1' subsite. Our findings showed compounds **18-20**, inhibiting the activity of MMP2 enzymes in the sub-nanomolar range, and displaying remarkable selectivity for MMP2 for **19** and **20**, as a consequence of the interaction with the zinc cation and key amino acids of the S1' catalytic subsite. Cell-based assays allowed to give insight about the effect of gelatinase inhibition of most active compounds **18-20**, suggesting that, in highly invasive and high MMPs-expressing melanoma cells, compounds **18** and **20** undertake their action reducing cell viability and invasiveness, while in low MMPs-expressing cells the same results were absent. Molecular docking calculations on compounds **18-20** within MMP2 and MMP9 active sites revealed the existence of a hydrophobic channel at the bottom of S1' subsite for MMP2, suggesting the rationale for the high selectivity experienced for compounds **19** and **20** in favour of such enzyme, and giving a tool for subsequent compound hit optimization.

Follow-up research is ongoing to study the inhibition profile on other MMP subtypes to assess inhibition selectivity within this class of enzymes, and to improve the inhibition profile of candidate peptidomimetics **19** and **20**, taking advantage of the binding mode of this compound towards MMP2. The development of D-proline-derived peptidomimetic compounds as gelatinase inhibitors may open the way for subsequent applications in molecular imaging of angiogenesis targeting the tumor microenvironment, and in further revisiting the possibility of developing chemotherapeutics for the treatment of early-stage cancer disease.

Experimental Section

General

Analytical grade solvents and commercially available reagents were used without further purification. Reactions requiring an inert atmosphere were carried out under a nitrogen atmosphere. Dry toluene was distilled over Na/benzophenone. Flash column chromatography (FCC) purifications were performed using Merck silica gel (40-63 μm). TLC analyses were performed on Merck silica gel 60 F254 plates. ^{1}H NMR spectra were recorded on a Varian Mercury 400 (^{1}H: 400 MHz),^{13}C spectra were recorded on a Varian Gemini 200 (^{13}C: 50 MHz). The chemical shifts (δ) and coupling constants (J) are expressed in parts per million (ppm) and hertz (Hz), respectively. Optical rotations were measured with JASCO DIP-360 digital polarimeter. Mass spectra were carried out by direct inlet on a LCQ Fleet^{TM} Ion Trap LC/MS system (Thermo Fisher Scientific) with an ESI interface in the positive mode.

General procedure for the synthesis of hydroxamic acids

Preparation of NH_2OK/NH_2OH solution: $NH_2OH{\cdot}HCl$ (8 eq) was solubilized in MeOH (0.4 mL/mmol) by heating to reflux until most of the salt was dissolved. The solution was cooled to <40 °C, and a solution of KOH (12 eq) in MeOH (0.2 mL) was added in one portion. The resulting suspension was cooled to room temperature before use and was added without prior removal of precipitated material to the methyl ester compound (1 eq) and stirred at room temperature for 16h. The reaction mixture was taken up in 1M HCl, extracted with EtOAc, dried over anhydrous Na_2SO_4, filtered, and concentrated under reduced pressure. Finally, the crude residue was purified by column chromatography.

*(R)-methyl 1-((3,4-dichlorophenyl)sulfonyl)pyrrolidine-2-carboxylate (**2**)*

In a dry round bottom flask, D-proline methyl ester hydrochloride (100 mg, 0.62 mmol) and DMAP (15 mg, 0.12 mmol) were added under nitrogen, followed by DCM (6 mL) and triethylamine (0.17 mL, 1.23 mmol). The solution was cooled in an ice bath and 3,4-dichlorobenzenesulfonyl chloride (245 mg, 0.72 mmol) was added portionwise, and then the reaction was left at room temperature for 16 h. Successively, the mixture was diluted with dichloromethane and washed with 1M HCl (3 x 20 mL), a saturated solution of $NaHCO_3$ (3 x 20 mL) and brine (20 mL). The organic solution was dried over Na_2SO_4 and concentrated on reduced pressure to obtain the product **2** as a yellow solid in a yield of 71%. $[\alpha]_D^{23}$ = + 65.1 ($CHCl_3$, *c* = 1.2). ^{1}H NMR (400 MHz, $CDCl_3$) δ 7.97 (dd, *J* = 1.9, 1.0 Hz, 1H), 7.71 (dd, *J* = 8.4, 2.1 Hz,1), 7.64 – 7.51 (m, 1H), 4.38 (dd, *J* = 8.5, 3.6 Hz, 1H), 3.76 – 3.65 (m, 4H), 3.48 – 3.29 (m, 2H), 2.22 – 2.06 (m, 1H), 2.05 – 1.99 (m, 2H), 1.88 (ddd, *J* = 9.3, 6.0, 3.9 Hz, 1H). ^{13}C NMR (100 MHz, $CDCl_3$) δ 172.2, 138.5, 137.6, 133.6, 131.0, 129.4, 126.5, 60. 5, 52.5, 48.3, 30.9, 24.7. MS (ESI) *m*/*z* (%) 360.17 (100, $[M + Na]^+$).

*(R)-1-((3,4-Dichlorophenyl)sulfonyl)-N-hydroxypyrrolidine-2-carboxamide (**3**)*

According to the general procedure, compound **3** was obtained in 36% yield from compound **2** (143 mg, 0.42 mmol) after flash chromatography on silica gel (DCM / MeOH = 30 : 1). $[\alpha]_D^{24}$ = + 108.5 ($CHCl_3$, *c* = 1.1). ^{1}H NMR (400 MHz, $CDCl_3$) δ 9.45 (br s, 1H), 7.96 (s, 1H), 7.67 (dd, *J* = 20.4, 7.6 Hz, 2H), 4.19 (s, 1H), 3.58 (s, 1H), 3.13 (s, 1H), 2.29 – 2.25 (m, 1H), 2.06 – 2.02 (m, 1H), 1.90 – 1.71 (m, 3H). ^{1}H NMR (400 MHz, $CDCl_3$) δ 168.7, 138.7, 135.4, 134.3, 131.5, 129.6, 126.7, 60.7, 49.8, 30.0, 24.3. MS (ESI) *m*/*z* (%) 361.17 (100, $[M + Na]^+$).

*(R)-Methyl 1-((4-methoxyphenyl)sulfonyl)pyrrolidine-2-carboxylate (**4**)*

In a dry round bottom flask, D-proline methyl ester hydrochloride (100 mg, 0.62 mmol) and DMAP (15 mg, 0.12 mmol) were added under nitrogen, followed by DCM (6 mL) and triethylamine (0.17

mL, 1.23 mmol). The solution was cooled in an ice bath and 4-methoxyphenylbenzenesulfonyl chloride (245 mg, 0.72 mmol) was added portionwise, then the reaction was left at room temperature for 16 h. Successively, the mixture was diluted with dichloromethane and washed with 1M HCl (3x 20 mL), a saturated solution of $NaHCO_3$ (3 x 20 mL) and brine (20 mL). The organic solution was dried over Na_2SO_4 and concentrated under reduced pressure to obtain product **4** as a yellow solid in a yield of 78%. $[\alpha]_D^{23}$ = + 61.7 ($CHCl_3$, *c* = 1.2). ^{1}H NMR (400 MHz, $CDCl_3$) δ 7.79 (d, *J* = 9.0 Hz, 2H), 6.97 (dd, *J* = 9.0, 1.0 Hz, 2H), 4.27 (dd, *J* = 8.0, 4.4 Hz, 1H), 3.85 (s, 3H), 3.71 (s, 3H), 3.51 – 3.37 (m, 1H), 3.31 – 3.20 (m, 1H), 2.10 – 1.83 (m, 3H), 1.82 – 1.63 (m, 1H). ^{13}C NMR (100 MHz, $CDCl_3$) δ 172.7, 163.0, 129.6, 114.2, 60.3, 55.6, 52.4, 48.4, 30.9, 24.7. MS (ESI) *m*/*z* (%) 322.20 (100, $[M + Na]^+$).

*(R)-N-Hydroxy-1-((4-methoxyphenyl)sulfonyl)pyrrolidine-2-carboxamide (**5**)*

According to the general procedure, compound **5** was obtained in 21% yield from compound **4** (140 mg, 0.22 mmol) after flash chromatography on silica gel (DCM / MeOH = 30 : 1). $[\alpha]_D^{21}$ = + 36.0 ($CHCl_3$, *c* = 0.85). ^{1}H NMR (400 MHz, $CDCl_3$) δ 7.79 (d, *J* = 8.0 Hz, 2H), 7.01 (d, *J* = 7.9 Hz, 2H), 4.17 (s, 1H), 3.88 (s, 3H), 3.52 (s, 1H), 3.14 (s, 1H), 2.24 (s, 1H), 1.82 (s, 1H), 1.67 – 1.52 (m, 2H). ^{13}C NMR (100 MHz, $CDCl_3$) δ 163.6, 130.0 (2C), 114.6 (2C), 55.7, 29.7 (2C), 24.0. MS (ESI) *m*/*z* (%) 323.20 (100, $[M+Na]^+$).

*(R)-Methyl 1-((4-bromophenyl) sulfonyl) pyrrolidine-2-carboxylate (**6**)*

In a dry round bottom flask under nitrogen flow, equipped with a magnetic stir bar, D-proline methyl ester hydrochloride (1000 mg, 6.17 mmol) and DMAP (150 mg, 1.23 mmol) was added under stirring, DCM (61 mL) and triethylamine (1.72 mL, 12.34 mmol). The solution was cooled in an ice bath, 4-bromobenzenesulfonyl chloride (2560 mg, 7.40 mmol) was added portionwise, then the reaction was left at room temperature for 16 h. Successively, the mixture was diluted with dichloromethane and washed with 1M HCl (3 x 60 mL), a saturated solution of $NaHCO_3$ (3 x 60 mL) and brine (60 mL). The organic solution was dried over Na_2SO_4 and concentrated under reduced pressure to obtain product **6** as a yellow solid in a yield of 85%. $[\alpha]_D^{23}$ = + 63.5 ($CHCl_3$, *c* = 1.1). **^{1}**H NMR (400 MHz, $CDCl_3$) 7.76 – 7.71 (m, 2H), 7.67 – 7.63 (m, 2H), 4.32 (dd, *J* = 8.4, 3.8 Hz, 1H), 3.69 (s, 3H), 3.44 (m, 1H), 3.32 (m, 1H), 2.14 – 1.89 (m, 3H), 1.88 – 1.74 (m, 1H). ^{13}C NMR (100 MHz, $CDCl_3$) δ 172.4, 137.5, 132.3, 129.0 (2C), 127.8 (2C), 60.4, 52.4, 48.32, 30.9, 24.7. MS (ESI) *m*/*z* (%) 436.25 (100, $[M + Na]^+$).

*(R)-Methyl 1-((4-(phenylethynyl)phenyl)sulfonyl)pyrrolidine-2-carboxylate (**7**)*

In a dry flask equipped with a magnetic stir bar CuI (27.3 mg, 0,14 mmol), **6** (250 mg, 0.72 mmol) and $Pd(PPh_3)_2Cl_2$ (76 mg, 0.15 mmol) were added under a nitrogen flow, and three nitrogen-vacuum cycles were performed. Successively, dry DMF (1.43 mL), triethylamine (600 µL, 4.30 mmol) and phenylacetylene (86 µL, 0.79 mmol) were added and the reaction mixture was stirred at 50 °C for 18 h. Then, the solution was diluted with ethyl acetate (30 mL) and washed with 5% NH_4OH (3 x 20 mL), 1M HCl (3 x 20 mL) and brine (20 mL), dried over Na_2SO_4 and concentrated under reduced pressure. The crude product was purified by Flash Chromatography (hexane / Et_2O = 2 : 1) to give the pure product as a yellow oil in 47% yield. $[\alpha]_D^{23}$ = + 83.5 ($CHCl_3$, *c* = 0.7). ^{1}H NMR (400 MHz, $CDCl_3$) δ: 7.85 (d, J = 8.5 Hz, 2H), 7.65 (d, *J* = 8.5 Hz, 2H), 7.55 (m, 2H), 7.39 – 7.32 (m, 3H), 4.34 (dd, *J* = 8.1, 4.0 Hz, 1H), 3.71 (s, 3H), 3.52-3.47 (m, 1H), 3.39 – 3.33 (m, 1H), 2.12 – 1.92 (m, 2H), 1.85 – 1.76 (m, 1H). ^{13}C NMR (100 MHz, $CDCl_3$) δ 172.4, 137.5, 132.0, 131.8 (2C), 129.0, 128.5

(2C), 128.1 (2C), 127.4 (2C), 122.4, 92.9, 87.8, 60.4, 52.4, 48.4, 30.9, 24.7. MS (ESI) *m*/*z* (%) 392.33 (100, $[M + Na]^+$).

*(R)-N-Hydroxy-1-((4-(phenylethynyl)phenyl)sulfonyl)pyrrolidine-2-carboxamide (**8**)*

Compound **8** was obtained following the general procedure starting from compound **7** (83 mg, 0.22 mmol). The crude product was purified by flash chromatography (only EtOAc) to give pure **8** in 31% yield. $[\alpha]_D^{24}$ = +102.8 ($CHCl_3$, *c* = 0.25). ^{1}H NMR (400 MHz, $CDCl_3$) δ 7.82 (d, *J* = 8.3 Hz, 1H), 7.70 (d, *J* = 8.4 Hz, 1H), 7.55 (m, 2H), 7.45 – 7.29 (m, 5H), 4.18 (d, *J* = 6.6 Hz, 1H), 3.74 - 3.70 (m, 1H), 3.59 - 3.56 (m, 1H), 3.29 (br s, 1H), 3.17 – 3.13 (m, 1H), 1.77 – 1.58 (m, 4H). ^{13}C NMR (50 MHz, DMSO-d_6) δ 173.0, 141.8, 137.4 (2C), 136.8 (2C), 134.7 (2C), 134.1 (2C), 132.9 (2C), 126.7, 93.1, 92.3, 64.6, 54.3, 35.9, 29.4. MS (ESI) *m*/*z* (%) 393.33 (100, $[M + Na]^+$).

*(R)-Methyl 1-((3',4'-dichloro-[1,1'-biphenyl]-4-yl)sulfonyl)pyrrolidine-2-carboxylate (**9**)*

In a dry Schlenk tube compound **6** (200 mg, 0.57 mmol), $Pd(PPh_3)_2Cl_2$ (59 mg, 0.09 mmol) and 3,4-dichlorophenyl)boronic acid (162 mg, 0.86 mmol) were added under a nitrogen atmosphere, and three nitrogen-vacuum cycles were performed. Then, degassed THF (2 mL) and a degassed 2M solution of Na_2CO_3 (1 mL) were added under a nitrogen flow and the resulting mixture was heated at 100 °C under microwave irradiation. After 1 h, the solution was diluted with ethyl acetate (30 mL) and washed with a saturated Na_2CO_3 solution (3 x 20 mL), 1M HCl (3 x 20 mL) and brine (20 mL), dried over Na_2SO_4 and concentrated under reduced pressure. The crude product was purified by flash chromatography (hexane / Et_2O = 1 : 1) to give the pure product in 75% yield. $[\alpha]_D^{19}$= + 30.8 ($CHCl_3$, *c* = 1.1) ^{1}H NMR (400 MHz, $CDCl_3$) δ 7.95 (d, *J* = 8.5 Hz, 2H), 7.68 (d, *J* = 8.5 Hz, 3H), 7.58 – 7.51 (m, 1H), 7.43 (dd, *J* = 8.3, 2.1 Hz, 1H), 4.38 (dd, *J* = 8.3, 3.9 Hz, 1H), 3.72 (s, 3H), 3.54 – 3.44 (m, 1H), 3.42 – 3.34 (m, 1H), 2.21 – 1.88 (m, 3H), 1.91 – 1.74 (m, 1H). ^{13}C NMR (100 MHz, $CDCl_3$) δ 172.5, 143.1, 139.3, 138.1, 133.3, 132.9, 131.1, 129.2 (2C), 128.3 (2C), 127.5, 126.5, 60.5, 52.5, 48.4, 31.0, 24.7. MS (ESI) *m*/*z* (%) 436.25 (100, $[M + Na]^+$).

*(R)-1-((3',4'-Dichloro-[1,1'-biphenyl]-4-yl)sulfonyl)-N-hydroxypyrrolidine-2-carboxamide (**10**)*

According to the general procedure, compound **10** was obtained in 39% yield from compound **9** (160 mg, 0.38 mmol) after flash chromatography on silica gel (EtOAc). $[\alpha]_D^{20}$ = + 141.0 ($CHCl_3$, *c* = 1.5). ^{1}H NMR (400 MHz, $CDCl_3$) δ 7.94 (d, *J* = 8.3 Hz, 2H), 7.76 – 7.63 (m, 3H), 7.56 (d, *J* = 8.3 Hz, 1H), 7.51 – 7.39 (m, 1H), 4.25 (d, *J* = 6.4 Hz, 1H), 3.62 - 3.58 (m, 1H) 3.22 - 3.16 (m, 1H), 2.25 (d, *J* = 11.7 Hz, 1H), 1.91 - 1.82 (m, 1H) 1.73-1.69 (m, 2H), ^{13}C NMR (100 MHz, $CDCl_3$) 168.6, 144.0, 138.8, 135.0, 133.4, 133.2, 132.8, 132.1, 131.1, 129.2, 128.6 (2C), 128.0 (2C), 126.5, 60.7, 49.8, 29.9, 24.3. MS (ESI) *m*/*z* (%) = 437.08 (100, $[M + Na]^+$).

*(R)-Methyl 1-((4-aminophenyl)sulfonyl)pyrrolidine-2-carboxylate: (R)-methyl 1-((4-nitrophenyl)sulfonyl)pyrrolidine-2-carboxylate (**12**)*

In a dry round bottom flask, D-proline methyl ester hydrochloride (1000 mg, 6.17 mmol) and DMAP (150 mg, 1.23 mmol) were added under a nitrogen atmosphere, followed by DCM (61 mL) and triethylamine (1.72 mL, 12.34 mmol). The solution was cooled in an ice bath and 4-nitrobenzenesulfonyl chloride (1639 mg, 7.40 mmol) was added portionwise, then the reaction was left at room temperature for 16 h. Successively, the mixture was diluted with dichloromethane and washed with 1M HCl (3 x 60 mL), a saturated solution of $NaHCO_3$ (3 x 60 mL) and brine (60 mL). The organic solution was dried over Na_2SO_4 and concentrated under reduced pressure to obtain product **11** as a yellow solid in 89% yield, with spectroscopical data in agreement with those reported

in literature.[28] To a solution of **11** (1900 mg, 6.05 mmol) in dry methanol (24 mL) 5% Pd/C (190 mg, 0.30 mmol) was added. Successively the round bottom flask was conditioned with H_2 and the reaction was left at room temperature. After 16 h, the mixture was filtered on celite and the solvent was removed under vacuum to give the pure product **12** as a yellow oil in a quantitative yield. $[\alpha]_D^{24}$ = + 89.4 ($CHCl_3$, *c* = 2.1). ^{1}H NMR (400 MHz, $CDCl_3$) δ 7.61 – 7.53 (m, 2H), 6.69 – 6.63 (m, 2H), 4.34 (br s, 2H), 4.18 – 4.16 (m, 1H), 3.67 (s, 3H), 3.45 – 3.41 (m, 1H), 3.25 – 3.16 (m, 1H), 2.00 – 1.84 (m, 3H), 1.75 – 1.60 (m, 1H). ^{13}C NMR (100 MHz, $CDCl_3$) δ 172.9, 151.2, 129.5 (2C), 125.3, 114.0 (2C), 60.3, 52.4, 48.5, 30.9, 24.6. MS (ESI) *m/z* (%) 307.27 (100, $[M + Na]^+$).

*(R)-Methyl 1-((4-benzamidophenyl)sulfonyl)pyrrolidine-2-carboxylate (**13**)*

In a dry round bottom flask, compound **12** (142 mg, 0.50 mmol) and DMAP (12.2 mg, 0.1 mmol) were added under a nitrogen atmosphere, followed by DCM (5 mL) and triethylamine (140 µL, 0.10 mmol). The solution was cooled in an ice bath and benzoyl chloride (84 mg, 0.6 mmol) was added dropwise, then the reaction was left at room temperature for 16 h. Successively, the mixture was diluted with dichloromethane and washed with 1M HCl (3 x 20 mL), a saturated solution of $NaHCO_3$ (3 x 20 mL) and brine (20 mL). The organic solution was dried over Na_2SO_4, concentrated under reduced pressure and purified by flash chromatography (EtPet / Et_2O = 1 : 2) to give pure **13** in 59% yield. ^{1}H NMR (400 MHz, $CDCl_3$) δ 7.88 – 7.81 (m, 1H), 7.77 – 7.66 (m, 3H), 7.54 – 7.41 (m, 2H), 7.41 – 7.26 (m, 4H), 4.30 (dd, *J* = 8.2, 3.9 Hz, 1H), 3.66 (s, 3H), 3.50 – 3.46 (m, 1H), 3.35 – 3.29 (m, 1H), 2.15 – 1.88 (m, 3H), 1.88 – 1.69 (m, 1H). ^{13}C NMR (100 MHz, $CDCl_3$) δ 173.2, 172.4, 144.2, 137.1, 134.1, 133.7, 132.9, 130.1, 129.3 (2C), 128.8, 128.7, 128.5, 128.0, 60.4, 52.5, 48.4, 30.9, 24.6. MS (ESI) *m/z* (%) 411.40 (100, $[M + Na]^+$).

*(R)-1-((4-Benzamidophenyl)sulfonyl)-N-hydroxypyrrolidine-2-carboxamide (**17**)*

According to the general procedure, compound **17** was obtained in 35% yield from compound **13** (140 mg, 0.36 mmol) after flash chromatography on silica gel (EtPet / EtOAc = 3 : 1). $[\alpha]_D^{24}$ = + 13.5 (DMSO, *c* = 3.4). ^{1}H NMR (400 MHz, DMSO-d_6) δ 8.03 (d, *J* = 8.7 Hz, 2H), 7.94 (t, *J* = 10.0 Hz, 2H), 7.83 (d, *J* = 8.7 Hz, 2H), 7.57 (dt, *J* = 28.1, 7.2 Hz, 3H), 3.89 (dd, *J* = 8.3, 4.1 Hz, 1H), 3.22 – 3.07 (m, 1H), 1.95 – 1.59 (m, 4H), 1.45 (td, *J* = 11.7, 5.8 Hz, 1H). ^{13}C NMR (100 MHz, DMSO-d_6) δ 168.4, 166.6, 143.9, 134.9, 132.4, 131.3, 128.9 (2C), 128.8 (2C), 128.3 (2C), 120.4 (2C), 59.9, 49.5, 31.1, 24.7. MS (ESI) *m/z* (%) 413.65 (100, $[M + Na]^+$).

*(R)-Methyl 1-((4-(4-nitrobenzamido)phenyl)sulfonyl)pyrrolidine-2-carboxylate (**14**)*

In a dry round bottom flask, compound **12** (100 mg, 0.35 mmol) and DMAP (5 mg, 0.04 mmol) were added under a nitrogen atmosphere, followed by DCM (1.5 mL) and triethylamine (74 µL, 0.53 mmol). The solution was cooled in an ice bath, a solution of *p*-nitrobenzoyl chloride (78 mg, 0.42 mmol) in DCM (0.5 mL) was added dropwise, then the reaction was left at room temperature for 16 h. Successively, the mixture was diluted with dichloromethane and washed with 1M HCl (3 x 20 mL), saturated $NaHCO_3$ solution (3 x 20 mL) and brine (20 mL). The organic solution was dried over Na_2SO_4, concentrated under reduced pressure and purified by flash chromatography (Petr.Et. / EtOAc = 1 : 1) to give the pure product in 43% yield. $[\alpha]_D^{23}$ = +11.7 (DMSO, *c* = 1.0). ^{1}H NMR (400 MHz, DMSO-d_6) δ 8.44 – 8.27 (m, 2H), 8.23 – 8.10 (m, 2H), 8.00 (d, *J* = 8.8 Hz, 2H), 7.81 (t, *J* = 7.1 Hz, 2H), 4.20 – 4.16 (m, 1H), 3.69 (s, 3H), 3.42 – 3.27 (m, 1H), 3.16 (dt, *J* = 9.6, 7.0 Hz, 1H), 1.97 – 1.74 (m, 3H), 1.66 – 1.46 (m, 1H). ^{13}C NMR (100 MHz, DMOS-d_6) δ 172.7, 165.1, 149.8, 143.3, 140.5, 132.3, 129.8 (2C), 128.8 (2C), 124.1 (2C), 120.8 (2C), 60.7, 52.6, 48.9, 30.8, 24.7. MS (ESI) m/z (%) 456.31 (100, $[M + Na]^+$).

*(R)-N-Hydroxy-1-((4-(4-nitrobenzamido)phenyl)sulfonyl)pyrrolidine-2-carboxamide (**18**)*

According to the general procedure, compound **18** was obtained in 29% yield from compound **14** (56 mg, 0.129 mmol) after flash chromatography on silica gel (EtOAc). $[\alpha]_D^{21}$ = + 15.3 (DMSO, *c* = 1.5). ^{1}H NMR (400 MHz, DMSO-d_6) δ 8.93 (s, 1H), 8.38 (d, *J* = 8.3 Hz, 2H), 8.19 (d, *J* = 8.7 Hz, 2H), 8.07 – 8.00 (m, 2H), 7.86 (d, *J* = 8.6 Hz, 2H), 3.94 – 3.84 (m, 1H), 3.37 (d, *J* = 6.4 Hz, 1H), 3.15 (d, *J* = 9.9 Hz, 1H), 1.86 – 1.62 (m, 4H), 1.49 – 1.37 (m, 1H). ^{13}C NMR (100 MHz, DMSO-d_6) δ 168.3, 165.0, 149.8, 143.4, 140.5, 131.9, 129.8 (2C), 128.9 (2C), 124.1 (2C), 120.6 (2C), 59.9, 49.5, 31.1, 24.7. MS (ESI) m/z (%) 457.40 (100, $[M + Na]^+$).

*(R)-Methyl 1-((4-(((benzyloxy)carbonyl)amino)phenyl)sulfonyl)pyrrolidine-2-carboxylate (**15**)*

In a dry round bottom flask, compound **12** (150 mg, 0.55 mmol) and DMAP (13.2 mg, 0.11 mmol) were added under a nitrogen atmosphere, followed by DCM (5.5 mL) and triethylamine (111 mg, 1.10 mmol). The solution was cooled in an ice bath, benzyl chloroformate (113 mg, 0.66 mmol) was added dropwise, and the reaction was left at room temperature for 16 h. Successively, the mixture was diluted with dichloromethane and washed with 1M HCl (3 x 20 mL), a saturated solution of $NaHCO_3$ (3 x 20 mL) and brine (20 mL). The organic solution was dried over Na_2SO_4 and concentrated under reduced pressure to obtain the product as a yellow oil in 58% yield. $[\alpha]_D^{21}$ = + 38.3 ($CHCl_3$, *c* = 0.9). ^{1}H NMR (400 MHz, $CDCl_3$) 7.78 (dd, *J* = 13.6, 8.8 Hz, 1H), 7.70 – 7.62 (m, 1H), 7.57 (d, *J* = 8.7 Hz, 1H), 7.43 – 7.34 (m, 6H), 7.2 (br s, 1H), 5.17 (s, 2H), 4.26 (ddd, *J* = 10.3, 8.0, 4.6 Hz, 1H), 3.71 (s, 3H), 3.54 – 3.42 (m, 1H), 3.31 – 3.24 (m, 1H), 2.14 – 1.87 (m, 3H), 1.73 (m, 1H). ^{13}C NMR (100 MHz, $CDCl_3$) δ 172.8, 155.1, 143.6, 142.3, 135.1, 129.6, 128.9, 128.7, 128.6, 128.5, 128.4, 128.0, 118.6, 118.1, 69.7, 60.4, 52.4, 48.5, 30.9, 24.6. MS (ESI) m/z (%) = 441.41 (100, $[M + Na]^+$).

*(R)-Benzyl-(4-((2-(hydroxycarbamoyl)pyrrolidin-1-yl)sulfonyl)phenyl)carbamate (**19**)*

According to the general procedure, compound **19** was obtained in 39% yield from compound **15** (131 mg, 0.22 mmol) after flash chromatography on silica gel (DCM / MeOH = 40 : 1). $[\alpha]_D^{21}$ = + 22.3 (DMSO, *c* = 2.2). ^{1}H NMR (400 MHz, DMSO-d_6) δ 8.92 (s, 1H), 7.75 (d, *J* = 8.9 Hz, 2H), 7.67 (d, *J* = 8.9 Hz, 2H), 7.39 (dtd, *J* = 18.8, 8.5, 4.3 Hz, 5H), 5.17 (s, 2H), 3.84 (dd, *J* = 8.4, 4.1 Hz, 1H), 3.18 – 3.00 (m, 2H), 1.83 – 1.56 (m, 4H), 1.55 – 1.32 (m, 1H). ^{13}C NMR (100 MHz, DMSO-d_6) δ 153.7, 143.8, 136.3, 130.2, 130.1, 129.0, 128.9, 128.6, 128.6, 118.2, 66.6, 59.6, 49.5, 31.1, 24.6. MS (ESI) *m/z* (%) 442.28 (100, $[M + Na]^+$).

*(R)-Methyl-1-((4-(4-((((benzyloxy)carbonyl)amino)methyl)benzamido)phenyl)sulfonyl) pyrrolidine-2- carboxylate (**16**)*

In a dry round bottom flask, compound **12** (150 mg, 0.55 mmol) and DMAP (13 mg, 0.11 mmol) were added under a nitrogen atmosphere, followed by DCM (5.5 mL) and triethylamine (111 mg, 1.10 mmol). The solution was cooled in an ice bath, benzyl 4-(chlorocarbonyl)benzylcarbamate (200 mg, 0.66 mmol), prepared as reported,[37] was added portionwise, then the reaction was left at room temperature for 16 h. Successively, the mixture was diluted with dichloromethane and washed with 1M HCl (3 x 20 mL), a saturated solution of $NaHCO_3$ (3 x 20 mL) and brine (20 mL). The organic solution was dried over Na_2SO_4 and concentrated under reduced pressure to obtain a crude mixture that was purified by Flash Chromatography (AcOEt / EtPet = 1 : 1) giving compound **16** as a yellow oil in 95% yield. $[\alpha]_D^{21}$ = 50.8 ($CHCl_3$, *c* = 1.2). ^{1}H NMR (400 MHz, $CDCl_3$) mixture δ 8.83 (br s, 0.5H), 8.03 (d, *J* = 8.2 Hz, 0.5H), 7.88 – 7.66 (m, 4H), 7.56 (d, *J* = 8.7 Hz, 0.5H), 7.43 – 7.16 (m, 8H), 6.63 (d, *J* = 8.7 Hz, 0.5H), 5.57 (br s, 1H), 5.13 and 5.11 (s, 2H), 4.45 – 4.36 (m, 2H), 4.28 –

4.13 (m, 1H), 3.68 (s, 3H), 3.51 – 3.34 (m, 1H), 3.23 (ddd, *J* = 16.5, 11.7, 7.2 Hz, 1H), 2.08 – 1.83 (m, 3H), 1.81 – 1.57 (m, 1H). ^{13}C NMR (400 MHz, $CDCl_3$) δ 13C NMR (101 MHz, cdcl3) δ 172.6, 166.0, 156.7, 143.1, 142.6, 136.3, 133.2, 132.6, 130.9, 129.6, 128.7, 128.6, 128.4, 128.2, 128.1, 128.0, 127.7, 127.6, 127.3, 120.1, 114.0, 67.0, 60.4, 52.5, 48.5, 46.3, 44.5, 30.9, 24.6. MS (ESI) *m/z* (%) 574.47 (100, $[M+Na]^+$).

*(R)-Benzyl 4-((4-((2-(hydroxycarbamoyl)pyrrolidin-1-yl)sulfonyl)phenyl)carbamoyl)benzylcarbamate (**20**)*

According to the general procedure, compound **20** was obtained in 33% yield from compound **16** (268 mg, 3.86 mmol) after flash column chromatography on silica gel (DCM / MeOH = 40 : 1). $[\alpha]_D^{22}$ = + 36.3 (DMSO, *c* = 1.2). ^{1}H NMR (400 MHz, DMSO-d_6) δ 8.02 (d, *J* = 8.8 Hz, 2H), 7.91 (d, *J* = 8.1 Hz, 2H), 7.82 (d, *J* = 8.6 Hz, 2H), 7.45 – 7.25 (m, 9H), 5.05 (s, 2H), 4.28 (d, *J* = 6.1 Hz, 1H), 4.21 (d, *J* = 5.9 Hz, 1H), 3.88 (dd, *J* = 8.3, 4.2 Hz, 1H), 3.14 (d, *J* = 9.9 Hz, 2H), 1.88 –1.61 (m, 4H). ^{13}C NMR (100 MHz, DMSO-d_6) δ 168.2, 166.4, 156.2, 139.7, 139.0, 137.4, 133.3, 128.8 (5C), 128.3 (2C), 128.2 (2C), 127.3 (2C), 120.3 (2C), 66.5, 58.0, 53.5, 49.7, 48.4, 44.5, 43.2, 27.7, 25.5. MS (ESI) *m/z* (%) 575.42 (100, $[M + Na]^+$).

Enzymatic inhibition assays

The inhibition potency of hydroxamic acid derivatives against MMP2 and MMP9 was assayed through a fluorometric assay using the fluorogenic substrate Mca-Lys-Pro-Leu-Gly-Leu-Dpa-Ala-Arg-NH_2 (Enzo life science). All the measurements were performed in 96-well plates with a BMG Labtech OptimaStar microplate reader. Excitation and emission wavelengths were 320 and 420 nm, respectively. All incubations were performed at 28 °C in 50 mM TrisHCl, 150 mM NaCl, 10 mM $CaCl_2$, 0.05% Brij35, 1% DMSO at pH 7.5. The inhibitors were pre-incubated with enzymes (1 nM) for 5 minutes at room temperature before the reaction was started by the addition of the fluorogenic substrate (3 μM). The decrease of fluorescence was monitored over 30 minutes (λ_{ex}=320 nm, λ_{em}=420 nm) at 28 °C. The percentages of inhibition for the test compounds were determined through the equation $(1-V_s/V_o)x100$, where V_s is the initial velocity in the presence of the inhibitor and V_o is the initial velocity of the unhibited reaction. The IC_{50} values were obtained by dose-response measurements using inhibitor range of concentrations 0.00001-20 μM and enzyme concentration equal to 1 nM. A detergent-based assay was used to determine the presence of promiscuous inhibitors.[38] All the experiments were performed in duplicate and data collected were analyzed using Graphpad 5.0 Software Package (Graphpad Prism, San Diego, CA).

Tridimensional structural alignment

The Swiss PDB viewer (SPDBV) program (4.0.1 version, Swiss Institute of Bioinformatics) was used to superimpose three dimensional structures of MMP2 (PDB: 1HOV) and MMP9 (PDB: 4H3X).[24] The two proteins were initially superimposed using the "magic fit". Then, with the "improve fit" option, SPDBV was asked to minimize the root-mean square distance (RMSD) using a least square algorithm. Structural alignment was generated after protein superimposition. Residues of the superimposed protein that were spatially close to residues of the static one were aligned. Appropriate gaps were inserted in the sequences to indicate a lack of structural correspondence.

Pairwise sequence alignment

Primary sequences of MMP2 (PDB: 1HOV) and MMP9 (PDB: 4H3X) were retrieved from the Protein Data Bank in FASTA format. EMBOSS water sequence alignment tool, EMBL-EBI,[25] was

used to carry out local alignments of the two proteins, by identifying local similarities in the two protein sequences using the Smith-Waterman algorithm.[39] EBLOSUM-62 substitution matrix was used and penalties of 10 and 0.5 were applied for gap opening and extension, respectively.

Docking Calculations

The selection of optimal MMP2 and MMP9 structures, as well as the optimization and validation of docking protocols were done with the MOE modeling suite.[40] The potential receptor structures were selected starting from two available PDBs for MMP2 (1QIB, 1HOV) and for MMP9 (1GKC, 4H3X).[41] All complexes were refined by using the QuickPrep tool of MOE,[40] which fixes eventual errors in the PDB file, protonates the protein at a pH=7 and performs a backbone-restrained geometry minimization. The docking protocol was optimized by evaluating the different options available in the MOE suite. Ligands were redocked in their native receptor and cross-docked to the other, to evaluate how critical was the starting receptor to reproduce the correct binding pose. The starting conformation of all ligands was scrambled by performing a low-mode conformational search, using the MMFF94x forcefield and the Born solvation model for water.[40] The optimal receptor structure and docking protocol were evaluated in their ability to reproduce the experimental binding pose of the evaluated ligand. The final protocol used MMP2 and MMP9 receptor models derived from 1HOV and 1GKC, respectively, even though an acceptable reproduction of the reference binding poses was also obtained with 1QIB and 4H3X. Triangle Matcher and London dG were selected as the placement algorithm and scoring function, respectively. The top 30 poses were refined by Induced Fit and rescored by the GBVI/WSA dG scoring functions.[42] The top 5 poses of the refined complexes were saved for visual inspection. Test ligands **5**, **18**-**20** were designed in MOE and subjected to a conformational search as mentioned above. The top conformation was used to prepare a ligand database for docking, which also included the 1HOV and 1GKC ligands (SC-74020 and a reverse hydroxamate inhibitor, respectively) for comparison. AM1-BCC charges[43] were computed and assigned to ligands before docking. All ligands were then docked to the MMP2 and MMP9 receptor models as described above.

The analysis of the binding mode of the docked conformations was carried out using PyMol software v0.99.[44]

Cell cultures

The melanoma cell line A375M6[45] was isolated from lung metastasis of SCID bg/bg mice i.v. injected human melanoma A375P line, obtained from American Type Culture Collection (ATCC, Rockville, MD). Human breast carcinoma MCF7 cell line, and colorectal carcinoma HCT116 cell line were obtained from American Type Culture Collection. Cancer cells were cultivated in Dulbecco's Modified Eagle Medium containing 4,5 mg/l glucose and 2 mM L-glutamine (high glucose DMEM 4500, Gibco), 48 supplemented with 10% fetal bovine serum (FBS, Euroclone, Milan, Italy), at 37 °C in a 10% CO2 humidified atmosphere as previously described.[46] Cells were harvested from subconfluent cultures by incubation with a trypsin-EDTA solution (Life Technologies), and propagated every 3 days. Cultures were periodically monitored for mycoplasma contamination using Chen's fluorochrome test.

Cell viability assay

Cell viability was assessed using both trypan blue exclusion (TBE) assay and MTT tetrazolium reduction assay (Sigma Aldrich, Milan, Italy). Briefly, for MTT assay, $5x10^4$ cells were plated into 96-multiwell plates in 0.2 mL of complete medium. After 24 h, culture medium was changed with

media containing different doses of the inhibitors. The plates were incubated for additional 24 h and at the end of the incubation culture media were removed and 0.2 mL of MTT reagent [3-(4,5-dimethylthiazol-2-yl)-2,5-diphenyltetrazolium bromide], diluted 0.5 mg/mL in medium without red phenol, were added to the wells. Plates were incubated at 37 °C for additional 1 h. Next, the MTT was removed and the blue MTT-formazan product was solubilized with dimethyl sulfoxide (DMSO) (Sigma Aldrich, Milan, Italy). The absorbance of the formazan solution was read at 595 nm using the microplate reader (ELX800, Biotek Instruments). Cell viability (MTT) is expressed as percentage compared to untreated cells. In parallel, $5x10^5$ cells were plated into 24-multiwell plates in complete medium. After 24 growth, culture medium was replaced with media containing different doses of the inhibitors. At the end of the incubation (24 h), cells were washed with PBS and re-suspended in 0.5 mL of complete medium. The suspensions were mixed 1:1 vol: vol with 0.4% trypan blue dye for 5 min at 25 °C, and cells were counted on a hemocytometer. Viable cells result unstained while nonviable-necrotic cells result stained. Cell viability (TBE) is expressed as percentage of viable-unstained cells of the total recorded and compared to untreated cells.

Invasion assay

Cells invasion was studied in Boyden chambers. Cells were loaded in the upper wells which were separated by 8 μm pore-size polycarbonate filters coated with Matrigel (12.5 μg/filter; BD Biosciences, Franklin Lakes, New Jersey) from the lower wells. Cells ($1x10^5$) were suspended in 200 μL of serum free medium and seeded in the upper compartment, the same medium was added in the lower chamber. Cells were incubated for 6 h at 37 °C, 10% CO_2 in air, in the presence of Ilomastat (10 μM), a MMPs inhibitor (Millipore, Billerica, Massachusetts) or compounds **18**-**20** at 1 μM or 10 μM. After incubation, filters were removed and the non-invading cells on the upper surface were wiped-off mechanically with a cotton swab. Cells on the lower side of the filters were fixed overnight in ice-cold methanol, and then stained using a DiffQuick kit (BD Biosciences) and pictures of randomly chosen fields were taken.

Statistical analysis

The experiments were performed at least three times for a reliable application of statistics. Statistical analysis was performed with GraphPad Prism software. Values are presented as mean ± SD. ANOVA or Student's T test were used to evaluate the statistical significance.

Acknowledgments

Financial support from MIUR (PRIN2015, cod. 20157WW5EH), Fondazione CR Firenze (cod. 2017.0721), CNR roadmap europea ESFRI:CISPIM and University of Florence are acknowledged.

References and notes

1. Cathcart, J.; Pulkoski-Gross, A.; Cao, J. *Genes Dis.* **2015**, *2*, 26-34
2. a) Burzlaff, N. Model Complexes for Zinc-Containing Enzymes. In: Concepts and Models in Bioinorganic Chemistry. Wiley-VCH, **2006**, pp. 397-429; b) McCawley, L. J.; Matrisian, L. M. *Mol. Med. Today* **2000**, *6*, 149-156; c) Werb, Z. *Cell* **1997**, *91*, 439-442; d) Birkedal-Hansen, H. *Curr. Opin. Cell. Biol.* **1995**, *7*, 728-735.
3. a) Johnson, G.; Galis, Z. S. *Arterioscler. Thromb. Vasc. Biol.* **2004**, *24*, 54-60; b) Visse, R.; Nagase, H. *Circ. Res.* **2003**, *92*, 827-839; c) Galis, Z. S.; Khatri, J. J. *Circ. Res*., **2002**, *90*, 251-262; d) Liu, Y. E.; Wang, M.; Greene, J.; Su, J.; Ullrich, S.; Li, H.; Sheng, S.; Alexander, P.; Sang, Q. A.; Shi, Y. E. *J. Biol. Chem.* **1997**, *272*, 20479-20483.

4. Raffetto, J. D.; Khalil, R. A. *Biochem. Pharmacol*. **2008**, *75*, 346-359.
5. a) Vihinen, P.; Ala-aho, R.; Kahari, V. M. *Curr. Cancer Drug Targets* **2005**, *5*, 203-220; b) Fingleton, B. *Expert Opin. Ther. Tar.* **2003**, *7*, 385-397; c) Yong, V. W.; Power, C.; Forsyth, P.; Edwards, D. R. *Nat. Rev. Neurosci*. **2001**, *2*, 502-511; d) George, S. J. *Expert Opin. Inv. Drug* **2000**, *9*, 993-1007; e) Yong, V. W. *Expert Opin. Inv. Drug* **1999**, *8*, 255-268.
6. Bergers, G.; Benjamin, L. E. *Nat. Rev. Cancer*, **2003**, *3*, 401-410; Itoh, T.; Tanioka, M.; Yoshida, H.; Yoshioka, T.; Nishimoto, H.; Itohara, S. *Cancer Res.*, **1998**, *58*, 1048-1051; Vu, T. H.; Shipley, J. M.; Bergers, G.; Berger, J. E.; Helms, J. A.; Hanahan, D.; Shapiro S. D.; Senior, R. M.; Werb, Z. *Cell*, **1998**, *93*, 411-422.
7. Bergers, G.; Brekken, R.; McMahon, G.; Vu, T. H.; Itoh, T.; Tamaki, K.; Tanzawa, K.; Thorpe, P.; Itohara, S.; Werb, Z.; Hanahan, D. *Nat. Cell Biol.*, **2000**, *2*, 737-744.
8. Mu, D.; Cambier, S.; Fjellbirkeland, L.; Baron, J. L.; Munger, J. S.; Kawakatsu, H.; Sheppard, D.; Broaddus, V. C.; Nishimura, S. L. *J. Cell. Biol.* **2002**, *157*, 493-507.
9. Egeblad M.; Werb, Z. *Nat. Rev. Cancer*, **2002**, *2*, 161-174.
10. a) Malaponte, G.; Zacchia, A.; Bevelacqua, Y.; Marconi, A.; Perrotta, R.; Mazzarino, M. C.; Cardile, V.; Stivala, F. *Oncol. Rep.*, **2010**, *24*, 81-87; b) Nikkola, J.; Vihinen, P.; Vuoristo, M. –S.; Kellokumpu-Lehtinen, P.; Kahari, V. –M.; Pyrhonen, S. *Clin. Cancer Res.* **2005**, *11*, 5158-5166.
11. Hofmann, U. B.; Westphal, J. R.; Waas, E. T.; Becker, J. C.; Ruiter D. J.; van Muijen, G. N. *J. Invest. Dermatol.*, **2000**, *115*, 625-632; b) Ray, J. M.; Stetler-Stevenson, W. G. *EMBO J.*, **1995**, *14*, 908-917.
12. a) Oshitari, T.; Okuyama, Y.; Miyata, Y.; Kosano, H.; Takahashi, H.; Natsugari, H. *Bioorg. Med. Chem.* **2011**, *19*, 7085-7092; b) Wang, J.; Medina, C.; Radomski, M. W.; Gilmer, J. F. *Bioorg. Med. Chem.* **2011**, *19*, 4985-4999; c) Fisher, J. F.; Mobashery, S. *Cancer Metastasis Rev.*, 2006, **25**, 115-; Li, N. G.; Shi, Z. H.; Tang, Y. P.; Duan, J. A. *Curr. Med. Chem.* **2009**, *16*, 3805-3827; d) Aureli, L.; Gioia, M.; Cerbara, I.; Monaco, F.; Fasciglione, G. F.; Marini, S.; Ascenzi, P.; Topai, A.; Coletta, M. *Curr. Med. Chem.* **2008**, *15*, 2192-2222; e) Dorman, G.; Kocsis-Szommer, K.; Spadoni, C.; Ferdinandy, P. *Recent Pat. Cardiovasc. Drug Discov.* **2007**, *2*, 186-194.
13. Natchus, M. G.; Bookland, R. G.; De, B.; Almstead, N. G.; Pikul, S.; Janusz, M. J.; Heitmeyer, S. A.; Hookfin, E. B.; Hsieh, L. C.; Dowty, M. E.; Dietsch, C. R.; Patel, V. S.; Garver, S. M.; Gu, F.; Pokross, M. E.; Mieling, G. E.; Baker, T. R.; Foltz, D. J.; Peng, S. X.; Bornes, D. M.; Strojnowski, M. J.; Taiwo, Y. O. *J. Med. Chem.*, **2000**, *43*, 4948-4963.
14. Scozzafava, A.; Supuran, C. T. *J. Med. Chem.* **2000**, *43*, 3677-3687
15. a) Tuccinardi, T.; Nuti, E.; Ortore, G.; Rossello, A.; Avramova, S. I.; Martinelli, A. *Bioorg. Med. Chem.* **2008**, *16*, 7749-7758; b) Hanessian, S.; MacKay, D. B.; Moitessier, N. *J. Med. Chem.* **2001**, *44*, 3074-3082.
16. Sandra A. Heitmeyer, Erin B. Hookfin, Lily C. Hsieh, Martin E. Dowty, Charles R. Dietsch, Vikram S. Patel, Susan M. Garver, Fei Gu, Matthew E. Pokross, Glen E. Mieling, Timothy R. Baker, David J. Foltz, Sean X. Peng, David M. Bornes, Michael J. Strojnowski, and Yetunde O. Taiwo Pavlaki, M.; Zucker, S. *Cancer Metastasis Rev.* **2003**, *22*, 177-203; Coussens, L. M.; Fingleton, B.; Matrisian, L. M. *Science* **2002**, *295*, 2387-2392.
17. a) Nuti, E.; Tuccinardi, T.; Rossello, A. *Curr. Pharm. Des.* **2007**, *13*, 2087-2100; b) Overall, C. M.; Kleifeld, O. *Nat. Rev. Cancer* **2006**, *6*, 227-239.
18. Vandenbroucke, R. E.; Libert, C. *Nat. Rev. Drug Discov.* **2014**, *13*, 904-927.

19. a) Sluijter, J. P.; de Kleijn, D. P.; Pasterkamp, G. *Cardiovasc. Res.* **2006**, *69*, 595-603; b) Deryugina, E. I.; Quigley, J. P. *Cancer Metastasis Rev.* **2006**, *25*, 9-34; c) Haas, T. L. *Can. J. Physiol. Pharmacol.* **2005**, *83*, 1-7.
20. Higashi, S.; Miyazaki, K. *Biol. Chem.* **2008**, *283*, 10068-10078; Overall, C. M.; Kleifeld, O. *Br. J. Cancer* **2006**, *94*, 941-946.
21. a) Beutel, B.;Song, J.; Konken, C. P.; Korpos, E.; Schinor, B.; Gerwien, H.; Vidyadharan, R.; Burmeister, M.; Li, L.; Haufe, G.; Sorokin, L. *Bioconj. Chem.* **2018**, *29*, 3715−3725; b) Bianchini, F.; Calugi, C.; Ruzzolini, J.; Menchi, G.; Calorini, L.; Guarna, A.; Trabocchi, A. *MedChemComm* **2015**, *6*, 277-282; c) Fabre, B.; Filipiak, K.; Zapico, J. M.; Díaz, N.; Carbajo, R. J.; Schott, A. K.; Martínez-Alcázar, M. P.; Suárez, D.; Pineda-Lucena, A.; Ramos, A.; de Pascual-Teresa, B. *Org. Biomol. Chem.* **2013**, *11*, 6623-6641; d) Zapico, J. M.; Serra, P.; García-Sanmartín, J.; Filipiak, K.; Carbajo, R. J.; Schott, A.K.; Pineda-Lucena, A.; Martínez, A.; Martín-Santamaría, S.; de Pascual-Teresa, B.; Ramos, A. *Org. Biomol. Chem.* **2011**, *9*, 4587-4599.
22. a) Fabre, B.; Ramos, A.; de Pascual-Teresa, B. *J. Med. Chem.* **2014**, *57*, 10205-10219; b) Fabre, B.; Filipiak, K.; Díaz, N.; Zapico J. M.; Suárez, D.; Ramos A.; de Pascual-Teresa, B. *ChemBioChem* **2014**, *15*, 399-412.
23. Calugi, C.; Trabocchi, A.; Lalli, C.; Guarna, A. *Eur. J. Med. Chem.*, 2012, **56**, 96-107.
24. a) Guex N, Peitsch M C. *Electrophoresis*, **1997**, 18, 2714-2723; b) ExPAsy Proteomics Server, http://www.expasy.org/spdbv/
25. a) http://www.ebi.ac.uk/Tools/psa/emboss_water/; b) EMBOSS Matcher - Pairwise Sequence Alignment from the EMBL-EBI tools website, http://www.ebi.ac.uk/Tools/psa/emboss_matcher/
26. Nicolotti, O.; Miscioscia, T. F.; Leonetti, F.; Muncipinto, G.; Carotti, A. *J. Chem. Inf. Model*, **2007**, 47, 2439-2448.
27. Ness, K. A.; Eddie, S. L.; Higgins, C. A.; Templeman, A.; D'Costa, Z.; Gaddale, K. K. D.; Bouzzaoui, S.; Mullan, P. B.; Williams, R. *Bioorg. Med. Chem. Lett.* **2015**, *25*, 5642-5645
28. Foschi, F.; Landini, D.; Lupi, V.; Mihali, V.; Penso, M.; Pilati, T.; Tagliabue, A. – *Chem. Eur. J.* **2010**, *16*, 10667-10670.
29. a) Köhrmann, A.; Kammerer, U.; Kapp, M.; Dietl, J.; Anacker, J. *BMC Cancer* **2009**, *9*, 188; b) Mitropoulou, T. N.; Tzanakakis, G. N.; Kletsas, D.; Kalofonos, H. P.; Karamanos, N. K. *Int. J. Cancer* **2003**, *104*, 155-160.
30. Araújo, R. F., Jr; Lira, G. A.; Vilaça, J. A.; Guedes, H. G.; Leitão, M. C.; Lucena, H. F.; Ramos, C. C. *Pathol. Res. Pract.* **2015**, *211*, 71-77.
31. Lu, C. C.; Chu, P. Y.; Hsia, S. M.; Wu, C. H.; Tung, Y. T.; Yen, G. C. *Int. J. Oncol.* **2017**, *50*, 736-744.
32. Peppicelli, S.; Bianchini, F.; Torre, E.; Calorini, L. *Clin. Exp. Metastasis* **2014**, *31*, 423-433.
33. Galardy, R. E.; Cassabonne, M. E.; Giese, C.; Gilbert, J..H.; Lapierre, F.; Lopez, H.; Schaefer, M. E.; Stack, R.; Sullivan, M.; Summers, B.; Tressler, R.; Tyrrel, D.; Wee, J.; Allen, S. D.; Castellot, J. J.; Barletta, J. P.; Schultz, G. S.; Fernando, L. A.; Fisher, S.; Cui, T. -Y.; Foellmer, H. G.; Grobelny, D.; Holleran, W. M. *Ann. NY Acad. Sci.* **1994**, *732*, 315-323.
34. Puyraimond, A.; Fridman, R.; Lemesle, M.; Arbeille, B.; Menashi, S. *Exp. Cell Res.* **2001**, *262*, 28-36.
35. Fowlkes, J. L.M.; Winkler, M. K. *Cytokine Growth Factor Rev.* **2002**, *13*, 277-287.
36. a) Chaput, L.; Mouawad, L. *J. Cheminform*. **2017**, *9*, 37; b) Huang, S. -Y.; Grinter, A. Z.; Zou, X. *Phys. Chem. Chem. Phys.* **2010**, *12*, 12899-12908.

37. Pawelczak, K.; Jones, T. R.; Kempny, M.; Jackman, A. L.; Newell, D. R.; Krzyzanowski, L.; Rzeszotarska, B. *J. Med. Chem*. **1989**, *32*, 160-165.
38. Feng, B. Y.; Shoichet, B. K. *Nat. Protoc*., 2006, **1**, 550-553.
39. Smith, T. F.; Waterman, M. S. *J. Mol. Biol.* **1981**, *147*, 195-197.
40. Molecular Operating Environment (MOE), 2018.01; Chemical Computing Group ULC, 1010 Sherbrooke St. West, Suite #910, Montreal, QC, Canada, H3A 2R7, 2018.
41. a) Antoni, C.; Vera, L.; Devel, L.; Catalani, M. P.; Czarny, B.; Cassar-Lajeunesse, E.; Nuti, E.; Rossello, A.; Dive, V.; Stura, E. A. *J. Struct. Biol.* **2013**, *182*, 246-254; b) Feng, Y.; Likos, J. J.; Zhu, L.; Woodward, H.; Munie, G.; McDonald, J. J.; Stevens, A. M.; Howard, C. P.; De Crescenzo, G. A.; Welsch, D.; Shieh, H. -S.; Stallings, W.C. *Biochim. Biophys. Acta* **2002**, *1598*, 10-23; c) Rowsell, S.; Hawtin, P.; Minshull, C. A.; Jepson, H.; Brockbank, S.; Barratt, D.; Slater, A. M.; Mcpheat, W.; Waterson, D.; Henney, A.; Pauptit, R.A. *J. Mol. Biol.* **2002**, *319*, 173-181; d) Dhanaraj, V.; Williams, M.G.; Ye, Q. -Z.; Molina, F.; Johnson, L. L.; Ortwine, D. F.; Pavlovsky, A.; Rubin, J. R.; Skeean, R. W.; White, A. D.; Humblet, C.; Hupe, D. J.; Blundell, T. L. *Croatica Chemica Acta* **1999**, *72*, 575-591.
42. Naïm, M.; Bhat, S.; Rankin, K. N.; Dennis, S.; Chowdhury, S. F.; Siddiqi, I.; Drabik, P.; Sulea, T.; Bayly, C. I.; Jakalian, A.; Purisima, E. O. *J. Chem. Inf. Model.* **2007**, *47*, 122-133.
43. Jakalian, A., Jack, D. B., Bayly, C. I. *J. Comput. Chem.* **2002**, *23*, 1623-1641.
44. DeLano, W. L. 'The PyMOL Molecular Graphics System.' DeLano Scientific LLC, San Carlos, CA, USA [http://www.pymol.org].
45. Peppicelli, S.; Bianchini, F.; Torre, E.; Calorini, L. *Clin. Exp. Metastasis* **2014**, *31*, 423-433.
46. Andreucci, E.; Peppicelli, S.; Carta, F.; Brisotto, G.; Biscontin, E.; Ruzzolini, J.; Bianchini, F.; Biagioni, A.; Supuran, C.T.; Calorini, L. *J. Mol. Med.* **2017**, *95*, 1341-1353.

Supplementary data

MTT and TBE assay results; copies of 1H and ^{13}C NMR data for all newly-synthesized compounds; cLogP data for hydroxamate compounds **3**, **5**, **8**, **10**, **17-20**; additional docking results for **5** and **18-20**; coordinates of MMP2 and MMP9 binding sites and of ligands. Supplementary data associated with this article can be found, in the online version, at http://dx.doi.org/10.1016